3.1: Introduction

Spiro compounds composed of cyclic structures fused at a central carbon atom have recently been the subject of considerable attention because of their interesting conformational features and their structural implications on biological systems. Compounds of this structural class represent an important group of naturally occurring substances that are characterized by their extensive biological properties and applications (Longeon *et al.* 1990). The spirooxindole ring system is the core structure in a variety of pharmacologically active agents and natural alkaloids (Trost and Brennan 2009). For example, pteropodine and isopteropodine have been shown to modulate the functions of muscarinic receptors in rats (Kang *et al.* 2002), whereas spirotryprostatin A and B have been identified as mammalian cell cycle inhibitors (**Figure 3.1.1**) (Cui *et al.* 1996).

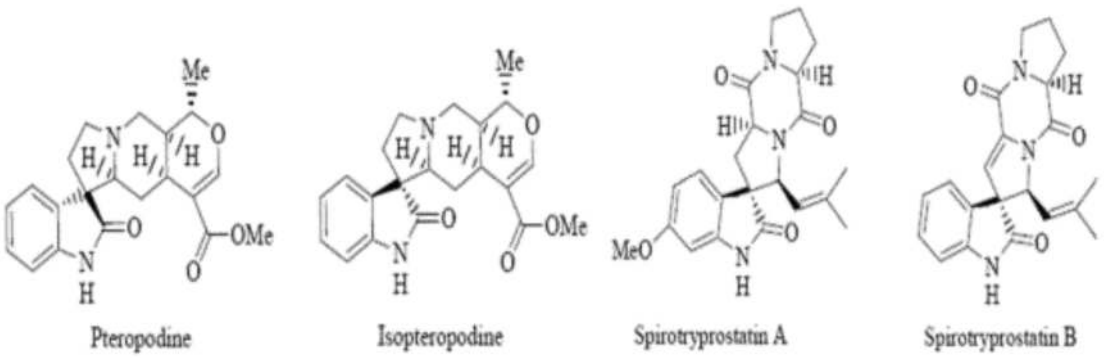

Figure 3.1.1: Bio-active spirooxindoles

The spirooxindole derivatives have also demonstrated significant potential for use in a wide range of biological applications such as antimicrobial (Bhaskar *et al.* 2012), antitumor (Jiang *et al.* 2012), and therapeutic agents (Galliford and Scheidt 2007). Of the heterocycles fused to a spirooxindole ring system, functionally substituted 4*H*-chromenes are of particular utility because they possess important biological activities.

Several methods have been developed for the synthesis of these heterocyclic skeletons. Isatin derivatives have been widely used in organic synthesis (Da Silva *et al.* 2001;Lashgari and Ziarani 2012), with one example including the preparation of spirooxindole derivatives via a three-component condensation

reaction of dimedone with activated methylene reagents in the presence of different catalysts such as $InCl_3$ (Shanthi *et al.* 2007), tetra-*n*-butylammonium fluoride (TBAF) (Gao *et al.* 2008), cyclodextrin (Sridhar *et al.* 2009), NH_4Cl (Dabiri *et al.* 2009), triethylbenzylammonium chloride (TEBA) (Zhu *et al.* 2007), ethylenediaminediacetate (EDDA) (Hari and Lee 2010), NaCl (Dandia *et al.* 2011), $HAuCl_4 \cdot 3H_2O$ (Kidwai *et al.* 2012), sodium stearate (Wang *et al.* 2010), L-proline (Li *et al.* 2010), triethylamine (Mortikov *et al.* 2008), MgO (Karmakar *et al.* 2012) and Carbon- SO_3H (Rao *et al.* 2013) as the catalysts. More recently, oxalic acid dihydrate: proline LTTM has been used for the synthesis of diverse spirooxindole derivatives at room temperature (Chandam *et al.* 2016)

Most of the reported methods are associated with the use of carcinogenic organic solvents, high temperatures, expensive and non-commercially available catalysts, or are lacking catalyst reusability. Thus there is great scope to develop a convenient and general approach towards the synthesis of substituted spirooxindoles from inexpensive, non-toxic and readily available reagents with improved yields in an ecofriendly fashion.

In recent years, mechanochemical methods such as ball-milling and grinding with pestle and mortar have emerged as a powerful techniques (Baig and Varma 2012;Bruckmann *et al.* 2008;James *et al.* 2012;Varma 2008). Among these, ball-milling has been a low-tech, low price, but more efficient mechanical method for the grinding of metals and inorganic substances into fine particles. Besides the broad applications of ball-milling in inorganic synthesis in the past decades (Baig and Varma 2012), the potential application and usefulness of ball-milling technology as a one-pot, solvent-free route in organic synthesis have largely been over looked. Actually, The mechanical energy generated by grinding of reactant materials results in the formation of new surfaces and cracks by breaking the order of the crystalline structure, and this results in the formation of products (Baig and Varma 2012).

Recently, nanostructured materials are used effectively as heterogeneous catalysts for various organic transformations, because they meet the goals of green and sustainable chemistry. Scientists and researchers have made considerable advances

in the synthesis of well defined nanostructured materials in past few decades. The ease of separation, recovery and reuse of nanoparticles further enhance their attractiveness as green and sustainable catalysts (Cox *et al.* 1988;Gladysz 2002;2001;Grunes *et al.* 2003;Pacchioni 2000;Polshettiwar *et al.* 2009;Polshettiwar *et al.* 2008;Polshettiwar and Varma 2010;Ramarao *et al.* 2002;Reetz and Westermann 2000).

ZrO_2 NPs have been extensively examined in the past decades due to their multiple potential applications (Liu and Lin 2005;Liu and Han 2010;Lu *et al.* 2008;Luo *et al.* 2006;Sholklapper *et al.* 2007;Steiner III *et al.* 2009). The crystal phase of ZrO_2 NPs (monoclinic or tetragonal) strongly influences the catalytic activities and selectivities (Rhodes and Bell 2005;Stichert *et al.* 2001). ZrO_2 nanoparticle catalyst as moisture stable, reusable, non-toxic, inexpensive and commercially available white powder is of great interest to many researchers in the recent years. In general, several similar applications of this nanoscale method, as an effective catalyst in green synthetic chemistry, have already been highlighted in the literature (Asakura *et al.* 1988;Chuah *et al.* 2000;Damyanova *et al.* 1997;He *et al.* 2004;Khodakov *et al.* 1999;Li *et al.* 2006;Mercera *et al.* 1990;Tsipouriari *et al.* 1994;Xie *et al.* 2000;Yamaguchi 1994).

In view of the above it was thought worthwhile to synthesize some novel substituted spirooxindoles via monoclinic ZrO_2 NPs catalysed one-pot three-component reaction of substituted isatin with 1, 3- dicarbonyl compounds and ethylcyanoacetate in a ball mill at room temperature.

3.2: Results and discussion

m-ZrO_2 NPs catalyzed multicomponent reaction of isatin derivatives **1a-h** with 1, 3-dicarbonyl compounds **2a-c** and ethylcyanoacetate **3** afforded substituted spirooxindoles **4a-r** in excellent yields under solvent free conditions in the ball mill at room temperature (**Scheme 3.2.1**). The chemical structures of the respective synthesized spirooxindoles were established by their spectral data.

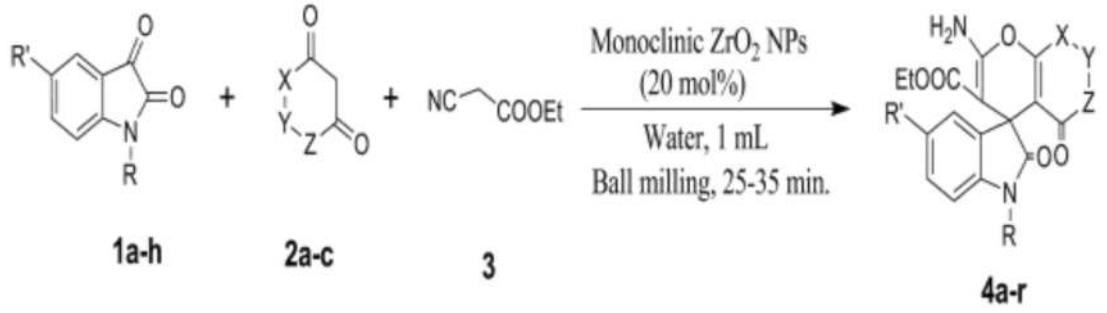

Scheme 3.2.1

In order to find optimum reaction conditions, several parameters were investigated in detail. First of all amount of catalyst (mol %) was examined. Therefore, a set of experiments using different amounts of *m*- ZrO_2 NPs were taken into account for the multicomponent reaction of 5-chlorisatin with ethylcyanoacetate and barbuteric acid (**Table 3.2.1**). The synthetic process was significantly dependent on the presence of catalyst and only poor yield was observed in the absence of catalyst after 150 min (**Entry 1, Table 3.2.1**). It was found that product yield is increased with enhancing catalyst concentration. Only 5 mol % of *m*- ZrO_2 NPs was sufficient to attain 56 % of product yield after 120 min (**Entry 2, Table 3.2.1**). The best yield of 97% was obtained with 20 mol % of *m*- ZrO_2 NPs (**Entry 7, Table 3.2.1**). However, further addition of catalyst concentration (> 20 mol%) did not improve the reaction rate and product yield (**Entry 8 and Entry 9**, **Table 3.2.1**).

Table 3.2.1: Effect of catalyst amount (mol %) on yield of the product **4a**

Entry	*m*-ZrO_2 mol%	Time(min)	%Yield
1	0	150	33
2	5	120	56
3	10	90	68
4	12	60	77
5	15	55	85
6	17	40	90
7	**20**	**30**	**97**
8	22	30	97
9	25	30	96

The effect of type of ZrO_2 (bulk, mixed phase nano, monoclinic nano) was investigated in the multicomponent reaction of 5-chloroisatin with ethylcyanoacetate and barbuteric acid under the optimized reaction conditions (**Table 3.2.2**). Four concentrations 5, 10, 15 and 20 mol% of ZrO_2 were used to study this important parameter. These data proved that particle size, surface area as well as a particular phase of ZrO_2 NPs is the important factor for its catalytic efficacy.

Table 3.2.2: Effect of type of ZrO_2 on the yield of the product **4a**

Type of ZrO_2	**Mol %**	**%Yield**
ZrO_2 (Bulk) Surface area: 6.95 m^2/g Average particle size: 2μm	5	40
	10	55
	15	59
	20	68
ZrO_2 (Mixed phase nano) Surface area: 44.70 m^2/g Average particle size: 20 nm	5	50
	10	60
	15	73
	20	83
ZrO_2 (single phase monoclinic) Surface area: 69.22 m^2/g Average particle size: >10 nm	5	56
	10	68
	15	85
	20	97

A comparison of the efficiency of catalytic activity of the *m*-ZrO_2 NPs with several other catalysts is presented in **table 3.2.3.** Multicomponent reaction of 5-chloroisatin with ethylcyanoacetate and barbuteric acid was taken into account and the comparison was in terms of mol % of catalyst, reaction time, and percentage yield. The result showed that *m*- ZrO_2 NPs was the best catalyst in terms of mol %, reaction time and percentage yield. Although some of the catalysts led to good yield, some of them are environmentally hazardous and require longer reaction time and higher mol % of catalyst (**Table 3.2.3**).Besides chemical variables, technical parameters like rotation frequency of ball mill and the number of milling balls also significantly influence the outcome of reactions performed in ball mills. Therefore, the influence of the rotation frequency on the yield of the product **4a** was investigated **(Table 3.2.4).** Another

critical parameter in ball-milling experiments is the number of milling balls. So far, the experiments were performed with 16 milling balls made of Al_2O_3 with a diameter *d* of 10 mm. **Table 3.2.5** summarize the results from experiments with number of milling balls varying from 2-18. It has to be stated expressly that a minimum of 10 milling balls are necessary to guarantee a quantitative yield of product **4a,** However the best yield of the product **4a** was obtained by using 16 milling balls under the optimized experimental conditions.

Table 3.2.3: Effect of different catalysts on the yield of the product **4a**

Entry	Type of catalyst	Mol %	Time (min.)	% Yield
1	Bentonite clay	20	200	70
2	K-10 clay	20	200	68
3	PTSA	30	200	51
4	NH_4Cl	30	165	60
5	EDTA	40	150	64
6	$Yb(OTf)_3$	20	120	72
7	TiO_2 (Nano)	20	50	82
8	$TiCl_3$	30	160	65
9	$MgClO_4$	30	120	50
10	DABCO	25	150	70
11	TEBA	25	180	76
12	$NaHCO_3$	40	220	72
13	K_2CO_3	40	150	69
14	TBAB	25	180	70
15	***m*-ZrO_2 NPs**	**20**	**30**	**97**

Table 3.2.4: Effect of rotation frequency of ball mill on the yield of the product **4a**

Entry	Rotation frequency (rpm)	% Yield
1	100	trace
2	200	55
3	300	70
4	400	75
5	500	85
6	600	88
7	700	93
8	**800**	**97**

Table 3.2.5: Effect of number of milling balls on the yield of the product **4a**

Entry	Number of Milling balls	% Yield
1	2	0
2	4	trace
3	6	20
4	8	35
5	10	60
6	12	80
7	14	88
8	**16**	**97**
9	18	97

Under the optimized set of reactions conditions, a number of isatin derivatives **1**, *viz.* 5-chloroisatin (**1a**), *N*-ethylisatin (**1b**), 5-chloro *N*-ethylisatin (**1c**), *N*-ethylacetaeisatin (**1d**), 5-chloro *N*-ethylacetaeisatin (**1e**), *N*-benzyliastin (**1f**), 5-

chloro *N*-benzylisatin (**1g**) and *N*-propylisatin (**1h**), were allowed to undergo multicomponent reaction with 1, 3 dicarbonylcompounds **2**, *viz*. barbuteric acid (**2a**), dimedone (**2b**) and meldrums acid (**2c**) andethylcyanoacetae **3**, in a molar ratio 1:1:1and 20 mol % of *m*- ZrO_2 NPs were placed to the milling beaker containing 16 milling balls. After that 1 ml water was added to the reaction mixture and the milling process was started. The progress of the reaction was monitored by thin layer chromatography. After the milling process, the beaker was opened and the milling balls were removed. Now 50 ml of acetone was added to the reaction mixture; the catalyst was removed and washed with several times by acetone. Then, the liquid portion was evaporated, dried and recrystallized with ethanol to yield pure substituted spirooxindoles **4,** *viz.*ethyl 7'-amino-5-chloro-2,2',4'-trioxo-1',2',3',4'-tetrahydrospiro[indoline-3,5'-pyrano[2,3 d]pyrimidine]-6'-carboxylate(**4a**), ethyl7'-amino-1-ethyl-2,2',4'-trioxo-1',2',3',4'-tetrahydrospiro [indoline-3,5'-pyrano[2,3 d]pyrimidine]-6'-carboxylate (**4b**), ethyl 7'-amino-5-chloro -1-ethyl-2,2',4'-trioxo-1',2',3',4'-tetrahydrospiro[indoline-3,5'-pyrano[2,3-d]pyrimidine]-6'-carboxylate (**3c**), ethyl 7'-amino-1-(2-ethoxy-2-oxoethyl)-2,2',4'-trioxo-1',2',3',4'-tetrahydrospiro[indoline-3,5'-pyrano[2,3d]pyrimidine]-6'-carboxylate (**4d**), ethyl 7'-amino-5-chloro-1-(2-ethoxy-2-oxoethyl)-2,2',4'-trioxo-1',2',3',4'tetrahydrospiro[indoline-3,5'-pyrano[2,3-d]pyrimidine]-6'-carboxylate(**4e**) ethyl 7'-amino-1-benzyl-2,2',4'-trioxo-1',2',3',4'-tetrahydrospiro [indoline-3,5'-pyrano[2,3-d]pyrimidine]-6'-carboxylate (**4f**), ethyl7'-amino-1-benzyl -5-chloro-2,2',4'-trioxo-1',2',3',4'-tetrahydrospiro[indoline-3,5'-pyrano[2,3-d]pyrimidine]-6'-carboxylate (**4g**), ethyl 7'-amino-2,2',4'-trioxo-1-propyl-1',2',3',4'-tetrahydrospiro [indoline-3,5'-pyrano[2,3-d]pyrimidine]-6'-carboxylate (**4h**), ethyl 2-amino-1'-ethyl -7,7-dimethyl-2',5-dioxo-5,6,7,8-tetrahydrospiro[chromene-4,3'-indoline]-3-carboxylate (**4i**), ethyl 2-amino-5'-chloro-1'-ethyl-7,7-dimethyl-2',5-dioxo-5,6,7, tetrahydrospiro[chromene-4,3'-indoline]-3-carboxylate (**4j**), ethyl 2-amino-1'-(2-ethoxy-2-oxoethyl)-7,7-dimethyl-2',5-dioxo-5,6,7,8 tetrahydrospiro[chromene-4,3'-indoline]-3-carboxylate (**4k**), ethyl 2-amino-5'-chloro-1'-(2-ethoxy-2-oxo ethyl)-7,7-dimethyl-2',5-dioxo-5,6,7,8-tetrahydrospiro[chromene-4,3'-indoline]-3-carboxylate (**4l**), ethyl 2-amino-7,7-dimethyl-2',5-dioxo-1'-propyl-5,6,7,8-tetra hydrospiro[chromene-4,3'-indoline]-3-carboxylate (**4m**), ethyl 7'-amino-1-ethyl-

2',2'-dimethyl-2,4'-dioxo-4'*H*-spiro[indoline-3,5'-pyrano[2,3-d][1,3]dioxine]-6'-carboxylate (**4n**), ethyl7'-amino-5-chloro-1-ethyl-2',2'-dimethyl-2,4'-dioxo-4'*H*-spiro[indoline-3,5'-pyrano[2,3-d][1,3]dioxine]-6'-carboxylate (**4o**), ethyl 7'-amino-1-(2-ethoxy-2-oxoethyl)-2',2'-dimethyl-2,4'-dioxo-4'*H*-spiro[indoline-3,5'-pyrano [2,3-d][1,3]dioxine]-6'-carboxylate (**4p**), ethyl 7'-amino-1-benzyl-2',2'-dimethyl-2,4'-dioxo-4'*H*-spiro[indoline-3,5'-pyrano[2,3-d][1,3]dioxine]-6'-carboxylate (**4q**), ethyl7'-amino-1-benzyl-5-chloro-2',2'-dimethyl-2,4'-dioxo-4'*H*-spiro[indoline-3,5'-pyrano[2,3-d][1,3]dioxine]-6'-carboxylate (**4r**). The results are given in the **table 3.2.6.**

Table 3.2.6: Synthesis of substituted spirooxindoles**(4a-r)**

Entry	Isatin derivatives	1,3 dicarbonyl compound	Product	%Yield	[a]Atom economy	Mp (^{0}C)
1	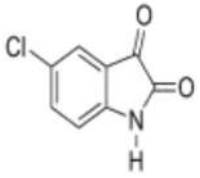 ***1a***	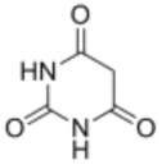 **2a**	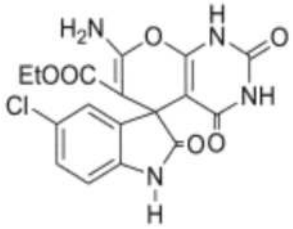 **4a**	97	93.9	246-248
2	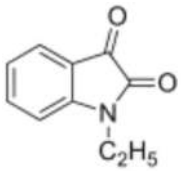 **1b**	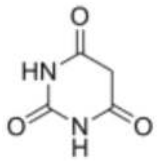 **2a**	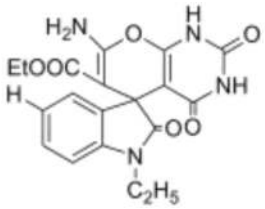 **4b**	96	95.7	210-212

3	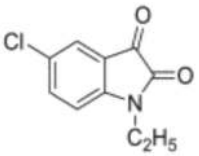 **1c**	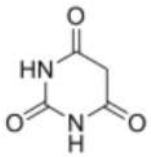 **2a**	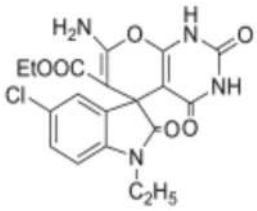 **4c**	97	96.2	206-208
4	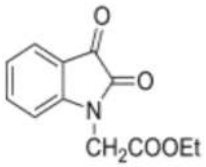 **1d**	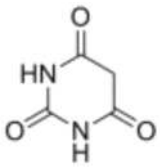 **2a**	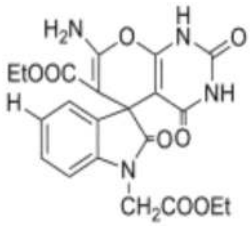 **4d**	91	96.3	204-206
5	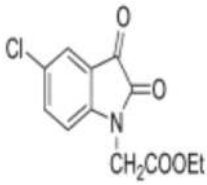 **1e**	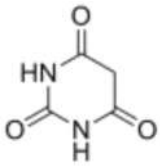 **2a**	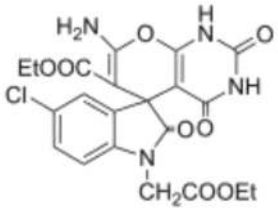 **4e**	93	96.6	212-214
6	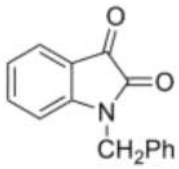 **1f**	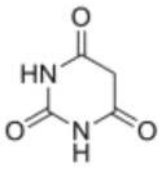 **2a**	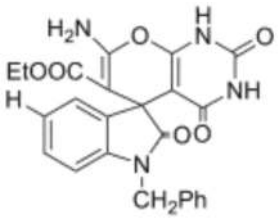 **4f**	94	96.3	228-230

7	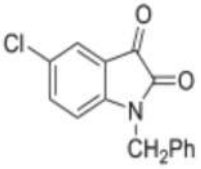 **1g**	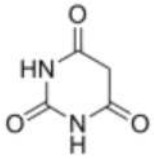 **2a**	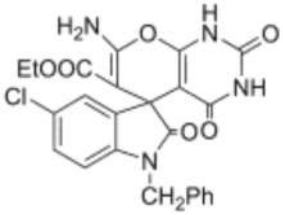 **4g**	95	96.6	254-256
8	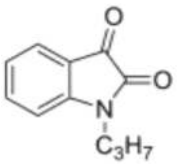 **1h**	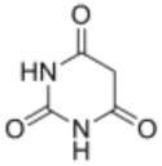 **2a**	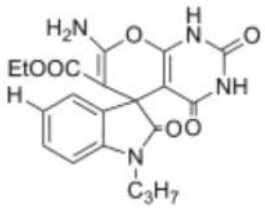 **4h**	90	95.9	198-200
9	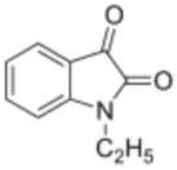 **1b**	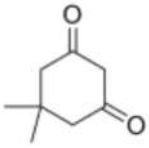 **2b**	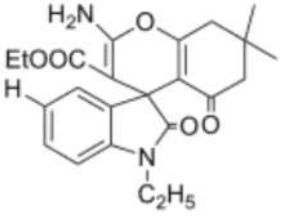 **4i**	96	95.9	260-262
10	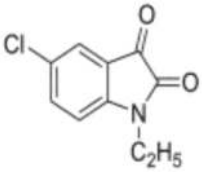 **1c**	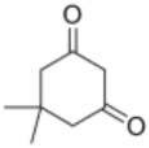 **2b**	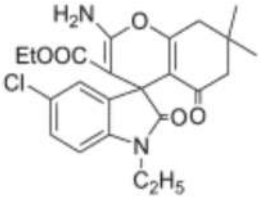 **4j**	96	96.3	270-272

11	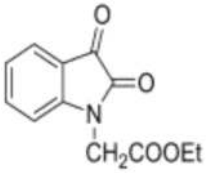 **1d**	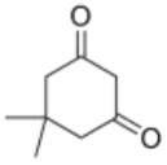 **2b**	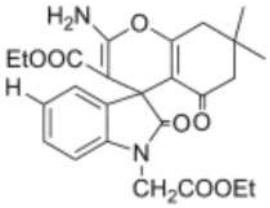 **4k**	95	96.4	222-224
12	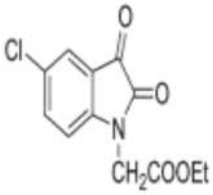 **1e**	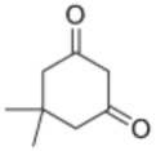 **2b**	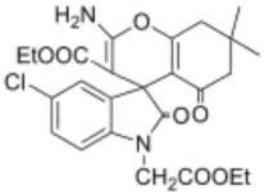 **4l**	92	96.7	252-254
13	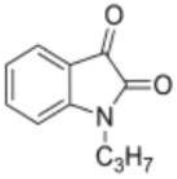 **1h**	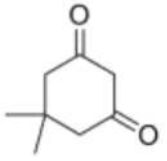 **2b**	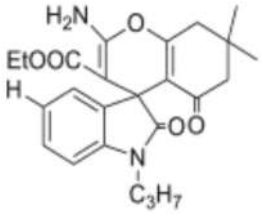 **4m**	89	95.9	236-238
14	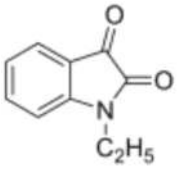 **1b**	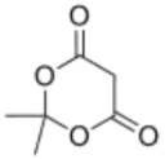 **2c**	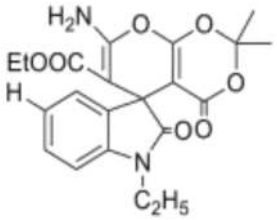 **4n**	90	95.9	110-112

15	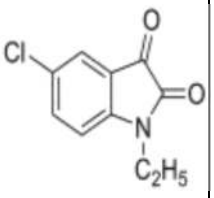 **1c**	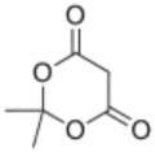 **2c**	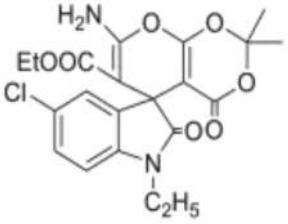 **4o**	88	96.3	165-167
16	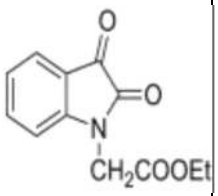 **1d**	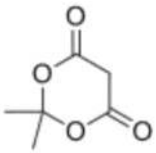 **2c**	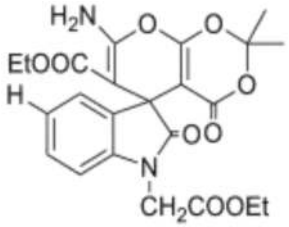 **4p**	82	96.5	202-204
17	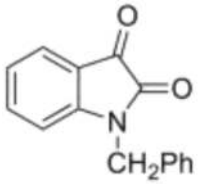 **1f**	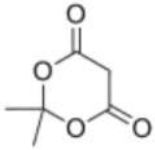 **2c**	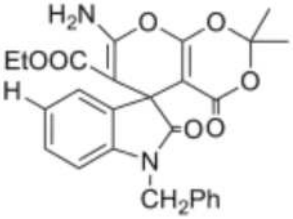 **4q**	86	96.4	182-184
18	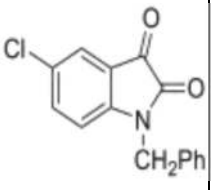 **1g**	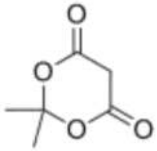 **2c**	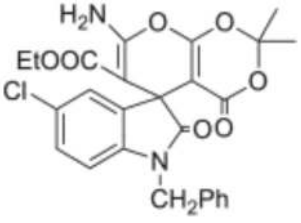 **4r**	88	96.7	194-196

[a]Atom economy = (molecular weight of desired product/sum of molecular weight of allreactants) × 100 %.

Traditionally, researchers have focused on maximizing yield or minimizing the number of steps. A high yield is desirable, but is not the whole story. Green chemistry and atom economy introduce a new goal into synthetic organic chemistry: designing reactions so that the atoms present in the starting materials end up in the product rather than in the waste stream. Atom economy means maximizing the incorporation of material from the starting materials or reagents into the final product. It is essentially pollution prevention at the molecular level. Atom economy is an important development beyond the traditionally taught concept of percent yield. In view of the above the atom economy of all products were calculated and summarized in the **table 3.2.6.**

A sequence of reactions such as Knoevenagel reaction, Michael reaction followed by Thorpe–Ziegler reaction takes place during the formation of the product. Mechanistically, the reaction was proposed to proceed through the activation of isatin derivatives **2** by *m*-ZrO_2 NPs **1** in order to generate α, β-unsaturated adduct **4**. Subsequent 1, 4-addition of 1,3-dione **5** on α, β-unsaturated adduct **4** followed by an intramolecular cyclization of the adduct through [1,3]-sigmatropic proton shift of the iminopyrans led to the formation of a stable spirooxindole ring system **10**. In the presence of both nitrile and ester groups, the nucleophilic addition of enolic oxygen occurs predominantly to nitrile rather than to the ester group affording the desired product. This predominance can be explained by the higher electrophilicity and lower steric hindrance of the nitrile group toward nucleophilic addition compared to ester functionality. Thus the formation of spirooxindole ring system is highly regioselective **(Scheme 3.2.2).**

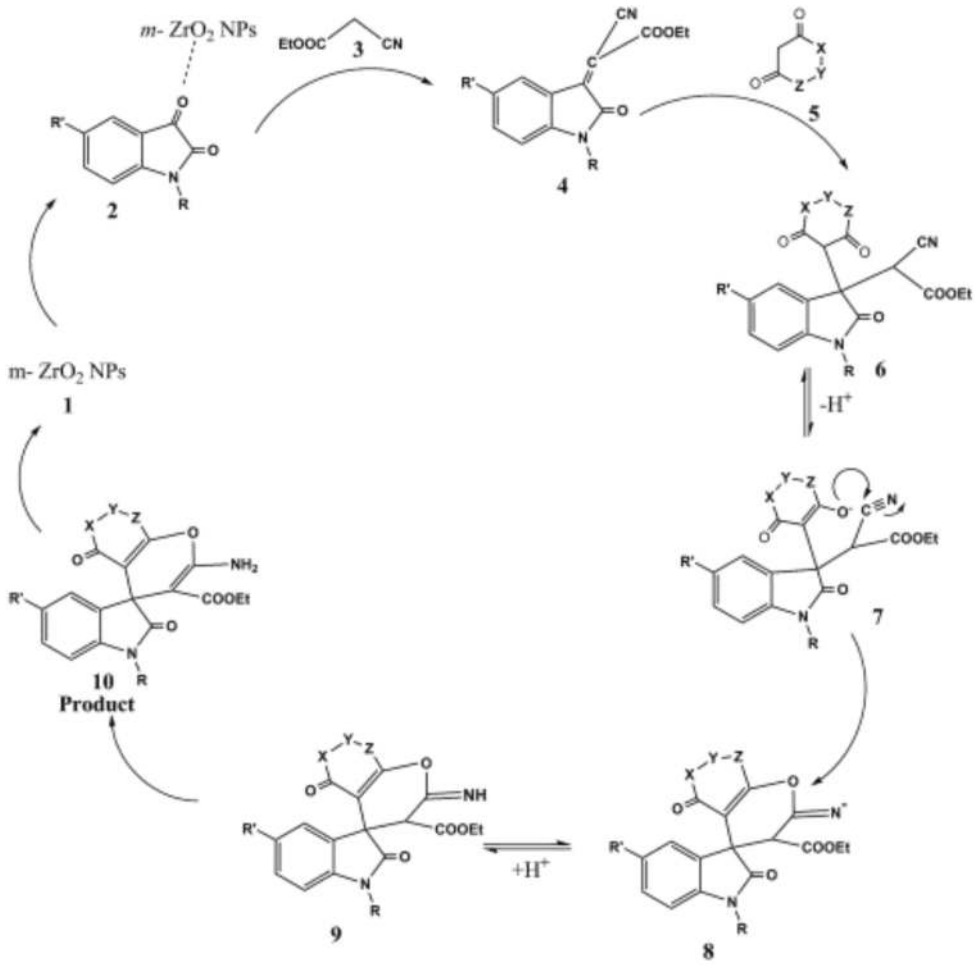

Scheme 3.2.2: Proposed mechanism for the formation of substituted spirooxindoles **4a-r**

m- ZrO_2 NPs were synthesized and characterized by FTIR, XRD, SEM and TEM analysis. The specific surface area of synthesized *m*-ZrO_2 NPs was calculated by BET surface area analyzer. It has been observed that the sample of *m*- ZrO_2 NPs was highly crystalline as evident from XRD pattern in which broad peaks with high intensity extended over the 2θ scale. The peaks observed at 2θ= 24.3 (011), 28.3 (11-1), 31.5 (111), 35.1 (200), 38.6 (021), 40.5 (21-1), 45.2 (20-2), 50.4 (122), 53.9 (300), 55.3 (013), 57.7 (22-2) and 60.0 (302) are corresponding to monoclinic zirconia (JCPDS card no. 37-1484). No characteristic peak of cubic or tetragonal phase and any other impurities are found in the XRD pattern. This observation suggests that the high purity of monoclinic phase ZrO_2 was obtained. The broadening of peaks indicates the smaller particle size of *m*-ZrO_2 NPs.

(Figure 3.2.1). The average particle size has been estimated by using *Debye-Scherer formula.*

$$D = 0.94 \lambda / \beta \cos\theta$$

Where, λ is wave length of X-Ray (0.1540 nm), β is FWHM (full width at half maximum), θ is diffraction angle and D is particle diameter size. On the basis of this investigation the average particle size was found 10 nm.

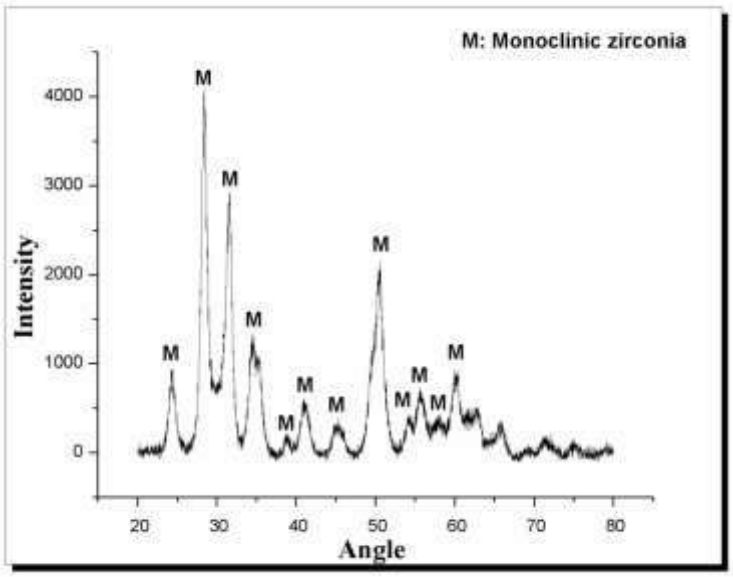

Figure 3.2.1: XRD spectra of *m*- ZrO_2 NPs

Further, the bonding nature and purity of nanoparticles are studied by the FT-IR. FT-IR spectra of *m*-ZrO_2NPs showed the presence of major bands at 774 and 481 cm^{-1} which are attributed to the strong stretching vibrations of the Zr–O group. These bands are the characteristic monoclinic phase of ZrO_2 (Rashad and Baioumy 2008). FT-IR studies are in agreement with the XRD patterns of the ZrO_2 that both confirm the presence of a monoclinic ZrO_2 phase.

Morphological investigations of 750 ^{0}C calcinated *m*- ZrO_2 NPs sample were carried out using SEM and TEM analysis that are shown in **Figure 3.2.2** and **Figure 3.2.3** respectively. It is clear from **Figure 3.2.2** that *m*- ZrO_2 particles are spherical in nature and size of the particles is in the nm regime, but size could not be finely resolved from SEM. For the purpose, TEM of sample has been shown in **Figure 3.2.3**.

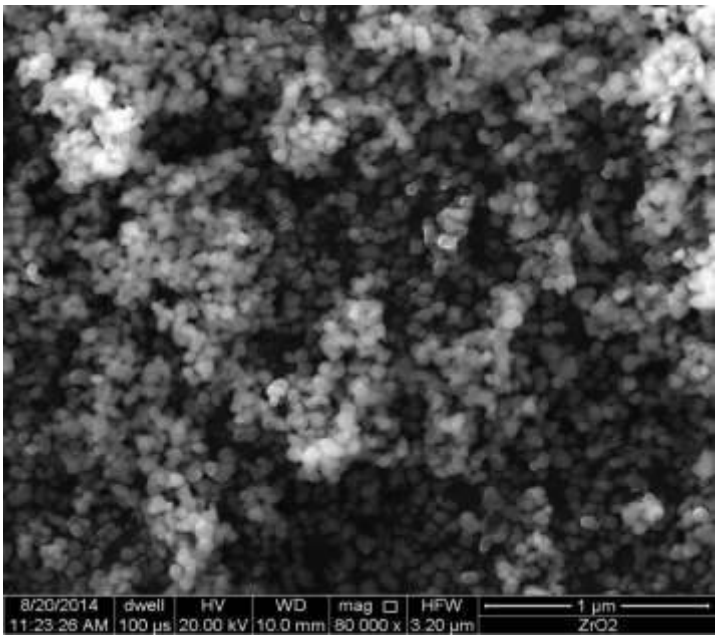

Figure 3.2.2: SEM image of *m*-ZrO_2 NPs

Transmission electron microscopy (TEM) analysis was carried out to confirm actual particle size of ZrO_2 NPs. Transmission electron microscopy (TEM) observations clearly revealed spherical nanoparticles with size ranging between 05–09 nm which is also in the agreement with XRD studies *m*- ZrO_2 NPs.

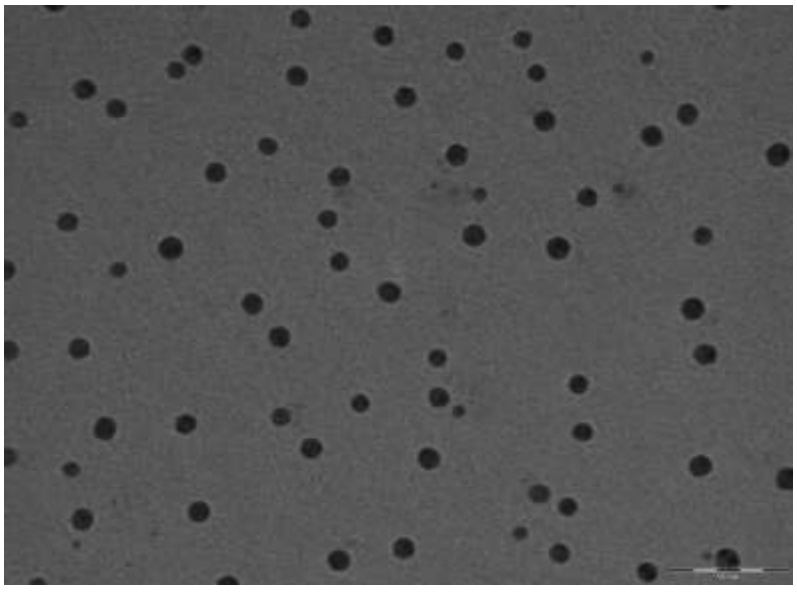

Figure 3.2.3: TEM image of *m*- ZrO_2 NPs

Surface area analysis of *m*- ZrO_2 NPs was done by nitrogen absorption using BET surface area analyzer and the surface area of synthesized *m*- ZrO_2 NPs was found to be 69. 22 m^2/g.

3.3: Experimental

3.3.1:Typical procedure for the synthesis of *m*- ZrO_2 NPs (Jafarpour *et al.* 2014)

A solution of $ZrOCl_2.8H_2O$ (0.003 mol) in distilled water was prepared. After that citric acid (0.126 mol) and ethylene glycol (0.126 mol) were subsequently added to this solution. The resulting mixture was stirred at 80 ^{0}C for 30 min to give rise to a clear solution. Now, the solution was refluxed at 95 ^{0}C for 12 h which turned it white, this is due to the formation of a metal–citrate homogeneous complex. After cooling down, in order to bring about the required chemical reactions for the development of polymerization and evaporation of the solvent, the sol was further slowly heated at 80 ^{0}C for 5 h in an open bath. During continuous heating at this temperature, the polymerization between citric acid, ethylene glycol and the complexes is developed, and ultimately the sol became more viscous as a wet gel. In the final step of the sol–gel process, the wet gel was fully dried by direct heating on the hot plate at 120 ^{0}C for 3 h. The resultant production was a light brown powder. Then it was calcined in a furnace at 750 ^{0}C for 4 h at a rate of 4 ^{0}C min in order to formation of white monoclinic nano zirconia powder.

3.3.2: General procedure for the synthesis of substituted spirooxindoles 4a-r

A milling beaker (100 ml) was equipped with 16 milling balls (Al_2O_3, *d*: 10 mm). Afterwards, isatin derivatives **1a-h** (0.01 mol), 1, 3- dicarbonyl compounds **2a-c** (0.01 mol), ethylcyanoacetate **3** (0.01 mol), water 1ml and 20 mol % of *m*- ZrO_2 NPs were placed to the milling beaker. The parameters, rotations per minute and milling time, were set-up and the milling process was started. The progress of the reaction was monitored by thin layer chromatography (n-hexane: ethyl acetate, 1:1). After the milling process, the beaker was opened and the milling balls were removed. Now 50 ml of acetone was added to the reaction mixture; the catalyst was removed by centrifuge and washed with several times by acetone. Then, the liquid portion was evaporated and dried. The crude products were recrystallized from ethanol.

Ethyl 7'-amino-5-chloro-2,2',4'-trioxo-1',2',3',4'-tetrahydrospiro[indoline-3, 5' pyrano[2,3-d]pyrimidine]-6'-carboxylate (4a)

Light yellowish white solid, **IR (KBr) υ**: 3395, 3305, 3112, 2955, 1729, 1698, 1688, 1632, 1623, 1611, 1570, 1458, 1368, 1284 cm^{-1}. **^{1}H NMR (300 MHz, DMSO) δ**: 1.19- 1.23 (t, *J*= 6.0 Hz, 3H, CH_3), 4.10- 4.17 (q, *J*= 7.2 Hz, 2H, CH_2), 6.86- 7.16 (m, 3H, aromatic protons), 7.34 (s, 2H, NH_2), 10.45 (s, 1H, NH), 11.09 (s, 1H, NH), 11.59 (s, 1H, NH) ppm. **^{13}C NMR (75.45 MHz, DMSO) δ**: 13.0, 46.2., 59.1, 76.2, 89.2, 108.1, 120.6, 122.7, 127.3, 135.3, 144.0, 149.1, 152.1, 158.6, 161.2, 167.4, 179.3 ppm. Anal. Calcd for $C_{17}H_{13}ClN_4O_6$: C, 50.45; H, 3.24; N, 13.84; O, 23.72 Found C, 50.38; H, 3.34; N, 13.80; O, 23.69.

Ethyl 7'-amino-1-ethyl-2,2',4'-trioxo-1',2',3',4'-tetrahydrospiro[indoline-3, 5' pyrano[2,3-d]pyrimidine]-6'-carboxylate (4b)

White solid, **IR (KBr) υ**: 3405, 3321, 3080, 2912, 2875, 1735, 1703, 1684, 1672, 1622, 1613, 1599, 1548, 1453, 1362, 1241 cm^{-1}. **^{1}H NMR (300 MHz, DMSO) δ**: 0.74- 0.78 (t, *J*= 6.9 Hz, 3H, CH_3), 1.02- 1.06 (t, *J*= 6.9 Hz, 3H, CH_3), 3.68- 3.71 (q, *J*= 3.6 Hz, 2H, CH_2), 4.50- 4.56 (q, *J*= 6.6 Hz, 2H, CH_2), 6.65- 7.07 (m, 4H, aromatic protons), 7.92 (s, 2H, NH_2), 10.21 (s, 1H, NH), 10.95 (s, 1H, NH) ppm. **^{13}C NMR (75.45 MHz, DMSO) δ**: 11.8, 13.4., 34.4, 45.9, 58.9, 75.2, 88.5, 123.0, 125.2, 127.2, 136.7, 143.4, 152.4, 158.9, 161.2, 167.1, 176.9 ppm. Anal. Calcd for $C_{19}H_{18}N_4O_6$: C, 57.28; H, 4.55; N, 14.06; O, 24.10 Found C, 57.15; H, 4.65; N, 14.10; O, 24.09.

Ethyl 7'-amino-5-chloro-1-ethyl-2,2',4'-trioxo-1',2',3',4'-tetrahydrospiro [indoline-3, 5'-pyrano[2,3-d]pyrimidine]-6'-carboxylate (4c)

White solid, **IR (KBr) υ**: 3334, 3261, 3120, 2971, 2863, 1724, 1702, 1691, 1669, 1618, 1607, 1607, 1600, 1448, 1361, 1255 cm^{-1}. **^{1}H NMR (300 MHz, DMSO) δ**: 0.63- 0.68 (t, *J*= 6.9 Hz, 3H, CH_3), 1.15- 1.19 (t, *J*= 6.9 Hz, 3H, CH_3), 3.56- 3.63 (q, *J*= 6.6 Hz, 2H, CH_2), 4.45- 4.62 (q, *J*= 7.2 Hz, 2H, CH_2), 6.81- 7.17 (m, 3H, aromatic protons), 7.96 (s, 2H, NH_2), 10.94 (s, 1H, NH), 11.04 (s, 1H, NH) ppm. **^{13}C NMR (75.45 MHz, DMSO) δ**: 11.9, 13.4., 34.3, 45.8, 58.8, 75.9, 89.2, 121.2, 122.7, 127.6, 134.6, 144.4, 149.1, 152.1, 158.8, 161.2, 167.3, 177.1 ppm. Anal.

Calcd for $C_{19}H_{17}ClN_4O_6$: C, 52.73; H, 3.96; N, 12.94; O, 22.18 Found C, 52.81; H, 3.90; N, 13.05; O, 22.20.

Ethyl 7'-amino-1-(2-ethoxy-2-oxoethyl)-2,2',4'-trioxo-1',2',3',4'-tetrahydrospiro[indoline-3, 5'-pyrano[2,3-d]pyrimidine]-6'-carboxylate (4d)

Yellowish white solid, **IR (KBr) υ**: 3442, 3351, 3211, 3110, 3000, 2615, 2861, 1730, 1726, 1710, 1694, 1677, 1622, 1610, 1606, 1565, 1458, 1332, 1212 cm^{-1}. **^{1}H NMR (300 MHz, DMSO) δ**: 0.54- 0.59 (t, *J*= 6.9 Hz, 3H, CH_3), 1.01- 1.06 (t, *J*= 7.2 Hz , 3H, CH_3), 3.67- 3.91 (dd, 2H, CH_AH_b), 4.11- 4.16 (q, *J*= 6.9 Hz, 2H, CH_2), 4.28- 3.49 (dd, 2H, CH_AH_b), 6.82- 7.16 (m, 4H, aromatic protons), 8.01 (s, 2H, NH_2), 10.95 (s, 1H, NH), 11.19 (s, 1H, NH) ppm. **^{13}C NMR (75.45 MHz, DMSO) δ**: 14.0, 14.1., 40.3, 42.5, 45.7, 58.6, 60.8, 75.6, 85.8, 121.8, 122.5, 127.4, 134.4, 144.3, 149.1, 152.1, 158.8, 161.1, 167.3, 167.9, 178.1 ppm. Anal. Calcd for $C_{21}H_{20}N_4O_8$: C, 55.26; H, 4.42; N, 12.28; O, 28.04 Found C, 55.30; H, 4.50; N, 12.19; O, 28.01.

Ethyl 7'-amino-5-chloro-1-(2-ethoxy-2-oxoethyl)-2,2',4'-trioxo-1',2',3',4' tetra hydrospiro[indoline-3,5'-pyrano[2,3-d]pyrimidine]-6'-carboxylate (4e)

Yellowish white, **IR (KBr) υ:** 3400, 3361, 3243, 3155, 3005, 2955, 2852, 1728, 1722, 1703, 1686, 1661, 1625, 1605, 1601, 1551, 1413, 1359, 1222 cm^{-1}. **^{1}H NMR (300 MHz, DMSO) δ:** 0.78- 0.83 (t, *J*= 6.9 Hz, 3H, CH_3), 1.03- 1.07 (t, *J*= 6.9 Hz, 3H, CH_3), 4.24- 4.31 (q, *J*=6.6 Hz, 2H, CH_2), 4.73- 4.80 (q, *J*= 6.9 Hz, 2H, CH_2), 5.1 (s, 2H, CH_2), 6.65- 6.68 (d, 1H, aromatic proton), 7.09 (s, 2H, aromatic proton), 8.00 (s, 2H, NH_2), 10.37 (s, 1H, NH), 10.99 (s, 1H, NH) ppm. **^{13}C NMR (75.45 MHz, DMSO) δ**: 13.1, 13.9., 46.5, 56.1, 59.2, 62.0, 75.6, 83.8, 123.1, 124.6, 127.1, 137.5, 143.0, 149.2, 152.5, 158.8, 161.3, 164.3, 167.3, 179.2 ppm. Anal. Calcd for $C_{21}H_{19}ClN_4O_8$: C, 51.39; H, 3.90; N, 11.41; O, 26.08 Found C, 51.50; H, 3.80; N, 11.30; O, 26.08.

Ethyl 7'-amino-1-benzyl-2,2',4'-trioxo-1',2',3',4'-tetrahydrospiro[indoline-3,5'-pyrano[2,3-d]pyrimidine]-6'-carboxylate (4f)

White solid, **IR (KBr) υ**: 3393, 3247, 3050, 2978, 1728, 1703, 1682, 1628, 1625, 1604, 1558, 1481, 1323, 1256 cm^{-1}. **^{1}H NMR (300 MHz, DMSO) δ**: 1.10- 1.14 (t, *J*= 6.9 Hz, 3H, CH_3), 4.42- 4.51 (m, 2H, CH_2), 5.01 (s, 2H, CH_2), 6.65- 6.67 (d, 2H, aromatic protons), 7.12- 7.15 (d, 1H, aromatic protons), 7.23- 7.31 (m, 4H, aromatic protons), 7.54- 7.51 (d, 2H, aromatic protons), 8.09 (s, 2H, NH_2), 11.10 (s, 1H, NH), 12.28 (s, 1H, NH) ppm. **^{13}C NMR (75.45 MHz, DMSO) δ**: 13.6, 44.1., 46.0, 56.0 79.3, 87.3, 123.0, 125.6, 127.1, 127.6, 128.2, 136.5, 136.8, 143.7, 149.0, 152.6, 158.8, 161.4, 167.1, 177.9 ppm. Anal. Calcd for $C_{24}H_{20}N_4O_6$: C, 62.60; H, 4.38; N, 12.17; O, 20.85 Found C, 62.62; H, 4.48; N, 12.10; O, 20.80.

Ethyl 7'-amino-1-benzyl-5-chloro-2,2',4'-trioxo-1',2',3',4'-tetrahydrospiro [indoline-3,5'-pyrano[2,3-d]pyrimidine]-6'-carboxylate (4g)

White solid, **IR (KBr) υ**: 3415, 3298, 3105, 3008, 2891, 1739, 1709, 1688, 1658, 1618, 1611, 1577, 1485, 1361, 1243 cm^{-1}. **^{1}H NMR (300 MHz, DMSO) δ**: 1.32- 1.36 (t, *J*= 6.6 Hz, 3H, CH_3), 4.37- 4.47 (m, 2H, CH_2), 4.91 (s, 2H, CH_2), 6.98- 8.17 (m, 10H, aromatic protons and NH_2), 9.30 (s, 1H, NH), 9.79 (s, 1H, NH) ppm. **^{13}C NMR (75.45 MHz, DMSO) δ**: 13.8, 42.9, 56.9, 63.2, 63.3, 80.2, 88.7, 118.2, 122.8, 127.2, 127.6, 128.7, 129.0, 135.5, 135.7, 144.0, 145.5, 155.1, 161.1, 164.0, 169.7, 179.7 ppm. Anal. Calcd for $C_{24}H_{19}ClN_4O_6$: C, 58.25; H, 3.87; N, 11.32; O, 19.40 Found C, 58.17; H, 3.85; N, 11.29; O, 19.43.

Ethyl 7'-amino-2,2',4'-trioxo-1-propyl-1',2',3',4'-tetrahydrospiro[indoline-3,5'-pyrano [2,3-d]pyrimidine]-6'-carboxylate (4h)

White solid, **IR (KBr) υ**: 3476, 3361, 3361, 3205, 2914, 2908, 2825, 1729, 1701, 1693, 1685, 1622, 1611, 1598, 1563, 1438, 1327, 1210 cm^{-1}. **^{1}H NMR (300 MHz, DMSO) δ**: 0.64- 0.68 (t, *J*= 6.9 Hz, 3H, CH_3), 0.92- 0.97 (t, *J*= 7.2 Hz, 3H, CH_3), 1.57- 1.68 (m, 2H, CH_2), 3.50- 3.68 (m, 4H, CH_2), 6.81- 7.16 (m, 4H, aromatic proton), 7.97 (s, 2H, NH_2), 10.94 (s, 1H, NH), 12.19 (s, 1H, NH) ppm. **^{13}C NMR (75.45 MHz, DMSO) δ**: 11.5, 13.4., 13.5, 20.3, 41.7, 45.9, 58.9, 75.3, 88.4, 122.9, 125.2, 127.2, 136.7, 144.0, 149.1, 152.4, 158.9, 161.2, 167.1, 177.3 ppm. Anal.

Calcd for $C_{20}H_{20}N_4O_6$: C, 58.25; H, 4.89; N, 13.59; O, 23.28 Found C, 58.33; H, 4.92; N, 13.51; O, 23.25.

Ethyl 2-amino-1'-ethyl-7,7-dimethyl-2',5-dioxo-5,6,7,8-tetrahydrospiro [chromene-4,3'-indoline]-3-carboxylate (4i)

White solid, **IR (KBr) υ**: 3248, 3203, 3005, 2981, 2978, 2838, 1731, 1710, 1684, 1659, 1626, 1607, 1600, 1566, 1452, 1371, 1245 cm^{-1}. **^{1}H NMR (300 MHz, DMSO) δ**: 0.65- 0.69 (t, *J*= 6.6 Hz, 3H, CH_3), 0.96 (s, 6H, CH_3), 1.07- 1.12 (t, *J*= 6.9 Hz, 3H, CH_3), 1.97- 2.12 (m, 2H, CH_2), 2.43- 2.56 (m, 2H, CH_2), 3.56- 3.65 (q, *J*= 9.0 Hz, 2H, CH_2), 4.43- 4.60 (q, *J*= 7.2 Hz, 2H, CH_2), 6.86- 7.19 (m, 6H, aromatic protons and NH_2) ppm. **^{13}C NMR (75.45 MHz, DMSO) δ**: 11.1, 16.5., 26.9, 27.6, 31.9, 34.2, 46.2, 49.8, 57.2, 72.5, 108.2, 117.0, 122.1, 122.9, 128.3, 133.7, 142.4, 158.8, 164.2, 169.6, 175.9, 194.8 ppm. Anal. Calcd for $C_{23}H_{26}N_2O_5$: C, 67.30; H, 6.38; N, 6.82; O, 19.49 Found C, 67.38; H, 6.40; N, 6.80; O, 19.51.

Ethyl 2-amino-5'-chloro-1'-ethyl-7, 7-dimethyl-2',5-dioxo-5,6,7, tetrahydro spiro[chromene-4, 3'-indoline]-3-carboxylate (4j)

White solid, **IR (KBr) υ**: 3321, 3215, 2999, 2977, 2911, 2822, 1737, 1701, 1689, 1672, 1635, 1614, 1605, 1570, 1478, 1343, 1249 cm^{-1}. **^{1}H NMR (300 MHz, DMSO) δ**: 0.75- 0.79 (t, *J*= 6.9 Hz, 3H, CH_3), 0.92- 1.00 (m, 9H, CH_3), 1.99- 2.12 (m, 2H, CH_2), 2.45- 2.49 (d, 2H, CH_2, mixed with DMSO peak), 3.30- 3.41 (m, 2H, CH_2 mixed with water peak), 3.66- 3.69 (q, *J*= 3.3 Hz, 2H, CH_2), 6.61- 6.64 (d, 1H, aromatic proton), 6.85 (s, 1H, aromatic proton), 7.02- 7.05 (d, 1H, aromatic proton), 7.87 (s, 2H, NH_2) ppm. **^{13}C NMR (75.45 MHz, DMSO) δ**: 11.8, 13.5., 26.6, 27.8, 31.5, 34.2, 46.1, 50.5, 58.5, 75.9, 106.9, 113.0, 121.0, 122.2, 127.4, 135.2, 144.3, 159.2, 162.4, 167.5, 177.5, 194.6 ppm. Anal. Calcd for $C_{23}H_{25}ClN_2O_5$: C, 62.09; H, 5.66; N, 6.30; O, 17.98 Found C, 62.00; H, 5.70; N, 6.29; O, 18.00.

Ethyl 2-amino-1'-(2-ethoxy-2-oxoethyl)-7,7-dimethyl-2',5-dioxo-5,6,7,8 tetra hydrospiro[chromene-4,3'-indoline]-3-carboxylate (4k)

White solid, **IR (KBr) υ**: 3361, 3222, 3012, 2971, 2913, 2844, 2834, 1739, 1737, 1708, 1691, 1678, 1628, 1609, 1606, 1555, 1453, 1341, 1250 cm^{-1}. **^{1}H NMR (300**

MHz, DMSO) δ: 0.54- 0.59 (t, *J*= 6.9 Hz, 3H, CH_3), 0.89 & 0.96 (two s, 6H, $2CH_3$), 1.17- 1.22 (t, *J*= 7.2 Hz, 3H, CH_3), 1.93- 2.11 (m, 2H, CH_2), 2.46-2.57 (m, 2H, CH_2, mixed with DMSO peak), 4.14- 4.21 (q, *J*= 6.6 Hz, 2H, CH_2), 4.44- 4.51 (q, *J*= 6.9 Hz, 2H, CH_2), 4.84 (s, 2H, CH_2), 6.79- 6.87 (m, 3H, aromatic protons), 7.07- 7.12 (t, 1H, aromatic proton), 7.90 (s, 2H, NH_2) ppm. **^{13}C NMR (75.45 MHz, DMSO) δ**: 15.0, 15.1., 27.0, 27.4, 31.5, 46.9, 50.5, 56.0, 58.9, 75.6, 109.3, 122.3, 124.3, 126.9, 138.1, 143.1, 159.1, 162.8, 167.4, 172.5, 179.5, 194.8 ppm. Anal. Calcd for $C_{25}H_{28}N_2O_7$: C, 64.09; H, 6.02; N, 5.98; O, 23.91 Found C, 64.15; H, 5.98; N, 6.05; O, 23.89.

Ethyl 2-amino-5'-chloro-1'-(2-ethoxy-2-oxoethyl)-7,7-dimethyl-2',5-dioxo-5,6,7,8-tetrahydrospiro[chromene-4,3'-indoline]-3-carboxylate (4l)

White Solid, **IR (KBr) υ**: 3334, 3241, 3023, 2934, 2921, 2822, 2817, 1741, 1734, 1701, 1698, 1684, 1625, 1615, 1603, 1561, 1449, 1340, 1259 cm^{-1}. **^{1}H NMR (300 MHz, DMSO) δ**: 0.65- 0.69 (t, *J*= 6.6 Hz, 3H, CH_3), 0.97 (s, 6H, CH_3), 1.27- 1.32 (t, *J*= 6.9 Hz, 3H, CH_3), 2.10 (s, 2H, CH_2), 2.45-2.57 (m, 2H, CH_2, mixed with DMSO peak), 4.14- 4.21 (q, *J*= 6.3 Hz, 2H, CH_2), 4.36- 4.43 (q, *J*= 6.9 Hz, 2H, CH_2), 4.78 (s, 2H, CH_2), 6.74- 6.76 (d, 1H, aromatic proton), 7.05 (s, 1H, aromatic proton), 7.12- 7.15 (d, 1H, aromatic proton), 7.27 (s, 2H, NH_2) ppm. **^{13}C NMR (75.45 MHz, DMSO) δ**: 15.1 16.6., 26.7, 27.8, 31.5, 41.6, 46.1, 50.5, 58.6, 76.1, 107.0, 121.1, 122.1, 127.4, 135.2, 144.9, 159.3, 162.5, 167.5, 171.4, 178.0, 194.7 ppm. Anal. Calcd for $C_{25}H_{27}ClN_2O_7$: C, 59.70; H, 5.41; N, 5.57; O, 22.27 Found C, 59.61; H, 5.50; N, 5.55; O, 22.34.

Ethyl 2-amino-7,7-dimethyl-2',5-dioxo-1'-propyl-5,6,7,8-tetrahydrospiro [chromene-4,3'-indoline]-3-carboxylate (4m)

White solid, **IR (KBr) υ**: 3290, 3209, 3150, 3028, 2920, 2910, 2852, 2840, 1739, 1707, 1680, 1671, 1618, 1611, 1598, 1548, 1458, 1342, 1224 cm^{-1}. **^{1}H NMR (300 MHz, DMSO) δ**: 0.64- 0.69 (t, *J*= 6.9 Hz, 3H, CH_3), 0.91-105 (m, 9H, CH_3), 1.61- 1.66 (t, *J*= 7.2 Hz, 2H, CH_2), 1.94- 2.14 (dd, 2H, CH_2), 2.43-2.60 (m, 2H, CH_2, mixed with DMSO peak), 3.41- 3.68 (m, 2H, CH_2 mixed with water peak), 4.35- 4.39 (t, *J*= 5.1 Hz, 2H, CH_2), 4.78 (s, 2H, CH_2), 6.78- 7.13 (m, 4H, aromatic

proton), 7.88 (s, 2H, NH_2) ppm. **^{13}C NMR (75.45 MHz, DMSO) δ**: 13.1, 18.5., 27.0, 27.4, 31.5, 46.9, 50.5, 56.0, 58.9, 75.6, 84.1, 109.3, 112.4, 122.3, 124.3, 126.9, 138.1, 143.1, 159.1, 162.8, 167.4, 179.5, 194.8 ppm. Anal. Calcd for $C_{24}H_{28}N_2O_5$: C, 67.91; H, 6.65; N, 6.60; O, 18.85 Found C, 67.99; H, 6.60; N, 6.65; O, 18.77.

Ethyl 7'-amino-1-ethyl-2',2'-dimethyl-2,4'-dioxo-4'H-spiro[indoline-3,5'-pyrano[2,3-d][1,3]dioxine]-6'-carboxylate (4n)

Brown solid, **IR (KBr) υ**: 3213, 3016, 2978, 2950, 2850, 2837, 1727, 1711, 1700, 1681, 1619, 1613, 1608, 1554, 1465, 1413, 1388, 1340, 1283, 1232 cm^{-1}. **^{1}H NMR (300 MHz, DMSO) δ**: 1.02- 1.06 (t, *J*= 6.9 Hz, 3H, CH_3), 1.30- 1.35 (t, *J*= 6.9 Hz, 3H, CH_3), 1.55 (s, 6H, CH_3), 4.05- 4.10 (q, *J*= 5.1 Hz, 2H, CH_2), 4.37-4.44 (q, *J*= 7.2 Hz, 2H, CH_2), 7.16-7.61 (m, 4H, aromatic protons), 8.25 (s, 2H, NH_2) ppm. **^{13}C NMR (75.45 MHz, DMSO) δ**: 12.2, 13.7, 24.9, 34.5, 46.4, 56.0, 75.6, 88.6, 105.0, 118.2, 122.6, 129.1, 135.9, 144.3, 145.6, 161.2, 163.4, 169.2, 180.1 ppm. Anal.Calcd for $C_{21}H_{22}N_2O_7$: C, 60.86; H, 5.35; N, 6.76; O, 27.03 Found C, 60.92; H, 5.40; N, 6.70; O, 26.98.

Ethyl 7'-amino-5-chloro-1-ethyl-2',2'-dimethyl-2,4'-dioxo-4'H-spiro[indoline-3,5'-pyrano[2,3-d][1,3]dioxine]-6'-carboxylate (4o)

Brown solid, **IR (KBr) υ**: 3271, 3058, 2996, 2960, 2861, 2844, 1735, 1708, 1695, 1680, 1623, 1610, 1605, 1572, 1487, 1450, 1377, 1341, 1228, 1220 cm^{-1}. **^{1}H NMR (300 MHz, DMSO) δ**: 1.12- 1.17 (t, *J*= 6.9 Hz, 3H, CH_3), 1.29- 1.34 (t, *J*= 7.2 Hz, 3H, CH_3), 1.64 (s, 6H, CH_3), 3.68- 3.75 (q, *J*= 7.2 Hz, 2H, CH_2), 4.37-4.44 (q, *J*= 6.9 Hz , 2H, CH_2), 7.02-7.55 (m, 3H, aromatic protons), 8.12 (s, 2H, NH_2) ppm. **^{13}C NMR (75.45 MHz, DMSO) δ**: 10.2, 11.9, 27.2, 27.5, 32.0, 47.1, 63.3, 74.9, 88.0, 110.2, 110.7, 117.2, 123.2, 125.6, 128.0, 136.4, 141.0, 146.2, 158.9, 164.6, 166.7, 177.8 ppm. Anal.Calcd for $C_{21}H_{21}ClN_2O_7$: C, 56.19; H, 4.72; N, 6.24; O, 24.95 Found C, 56.20; H, 4.70; N, 6.20; O, 24.94.

Ethyl 7'-amino-1-(2-ethoxy-2-oxoethyl)-2',2'-dimethyl-2,4'-dioxo-4'H-spiro [indoline-3,5'-pyrano[2,3-d][1,3]dioxine]-6'-carboxylate (4p)

Brown solid, **IR (KBr) υ**: 3317, 3103, 2990, 2971, 2838, 2828, 1737, 1731, 1713, 1693, 1684, 1615, 1609, 1607, 1569, 1448, 1431, 1351, 1322, 1255, 1232 cm^{-1}. **^{1}H NMR (300 MHz, DMSO) δ**: 1.01- 1.06 (t, *J*= 6.9 Hz, 3H, CH_3), 1.17- 1.21 (t, *J*= 6.9 Hz, 3H, CH_3), 1.63 (s, 6H, CH_3), 4.36- 4.43 (q, *J*= 6.9 Hz, 2H, CH_2), 4.51-4.56 (q, *J*= 6.6 Hz, 2H, CH_2), 6.65-7.23 (m, 4H, aromatic protons), 7.98 (s, 2H, NH_2) ppm. **^{13}C NMR (75.45 MHz, DMSO) δ**: 13.1, 13.9, 24.5, 46.5, 56.1, 59.2, 62.0, 75.7, 88.6, 109.4, 110.7, 123.0, 124.7, 127.1, 137.5, 143.0, 149.2, 152.5, 158.8, 161.3, 164.3, 167.2, 179.3 ppm. Anal.Calcd for $C_{23}H_{24}N_2O_9$: C, 58.47; H, 5.12; N, 5.93; O, 30.48 Found C, 58.47; H, 5.10; N, 5.90; O, 30.55.

Ethyl 7'-amino-1-benzyl-2',2'-dimethyl-2,4'-dioxo-4'H-spiro[indoline-3,5'-pyrano[2,3-d][1,3]dioxine]-6'-carboxylate (4q)

Brown solid, **IR (KBr) υ**: 3317, 3200, 2999, 2955, 2947, 2833, 2827, 1729, 1700, 1693, 1684, 1630, 1611, 1606, 1571, 1458, 1423, 1388, 1343, 1266, 1208 cm^{-1}. **^{1}H NMR (300 MHz, DMSO) δ**: 0.94- 0.98 (t, *J*= 7.2 Hz, 3H, CH_3), 1.64 (s, 6H, CH_3), 4.08- 4.14 (q, *J*= 6.6 Hz, 2H, CH_2), 4.44 (s, 2H, CH_2), 6.13-7.09 (m, 9H, aromatic protons), 7.51 (s, 2H, NH_2) ppm. **^{13}C NMR (75.45 MHz, DMSO) δ**: 13.6, 25.1., 44.1, 45.8, 58.8, 76.2, 88.8, 107.6, 121.5, 122.6, 127.0, 127.4, 127.6, 128.1, 134.6, 136.9, 144.7, 149.0, 152.4, 158.7, 161.3, 167.2, 178.1 ppm.Anal. Calcd for $C_{26}H_{24}N_2O_7$: C, 65.54; H, 5.08; N, 5.88; O, 23.50 Found C, 65.49; H, 5.10; N, 5.85; O, 23.56.

Ethyl 7'-amino-1-benzyl-5-chloro-2',2'-dimethyl-2,4'-dioxo-4'H-spiro[indoline -3,5'-pyrano[2,3-d][1,3]dioxine]-6'-carboxylate (4r)

Brown solid, **IR (KBr) υ**: 3351, 3213, 3021, 2948, 2927, 2817, 2812, 1731, 1703, 1688, 1678, 1626, 1610, 1600, 1569, 1453, 1408, 1361, 1311, 1290, 1213 cm^{-1}. **^{1}H NMR (300 MHz, DMSO) δ**: 1.05- 1.10 (t, *J*= 7.2 Hz, 3H, CH_3), 1.6 (s, 6H, CH_3), 4.10- 4.17 (q, *J*= 7.2 Hz, 2H, CH_2), 4.99 (s, 2H, CH_2), 6.75 (s, 1H, aromatic proton), 7.21-7.43 (m, 7H, aromatic protons), 7.69 (s, 2H, NH_2) ppm. **^{13}C NMR (75.45 MHz, DMSO) δ**: 13.9, 24.9., 46.5, 56.1, 59.2, 75.7, 88.6, 106.1, 123.8,

125.8, 126.1, 128.8, 128.9, 130.4, 130.8, 135.2, 141.9, 144.6, 144.7, 161.1, 162.5, 162.7, 164.9, 167.3, 179.2 ppm. Anal.Calcd for $C_{26}H_{23}ClN_2O_7$: C, 61.12; H, 4.54; N, 5.48; O, 21.92 Found C, 61.12; H, 4.54; N, 5.48; O, 21.92.

3.4: References

Asakura, K., Aoki, M., Iwasawa, Y., Selective isopentane formation from CH3OH on a new one-atomic layer ZrO2/ZSM-5 hybrid catalyst, Catalysis letters, 1, 395-403, 1988.

Baig, R. N., Varma, R. S., Alternative energy input: mechanochemical, microwave and ultrasound-assisted organic synthesis, Chemical Society Reviews, 41, 1559-1584, 2012.

Bhaskar, G., Arun, Y., Balachandran, C., Saikumar, C., Perumal, P. T., Synthesis of novel spirooxindole derivatives by one pot multicomponent reaction and their antimicrobial activity, European journal of medicinal chemistry, 51, 79-91, 2012.

Bruckmann, A., Krebs, A., Bolm, C., Organocatalytic reactions: effects of ball milling, microwave and ultrasound irradiation, Green Chemistry, 10, 1131-1141, 2008.

Chandam, D. R., Mulik, A. G., Patil, D. R., Deshmukh, M. B., Oxalic acid dihydrate: proline as a new recyclable designer solvent: a sustainable, green avenue for the synthesis of spirooxindole, Research on Chemical Intermediates, 42, 1411-1423, 2016.

Chuah, G., Liu, S., Jaenicke, S., Li, J., High surface area zirconia by digestion of zirconium propoxide at different pH, Microporous and mesoporous materials, 39, 381-392, 2000.

Cox, D., Trevor, D., Whetten, R., Kaldor, A., Aluminum clusters: ionization thresholds and reactivity toward deuterium, water, oxygen, methanol, methane, and carbon monoxide, The Journal of Physical Chemistry, 92, 421-429, 1988.

Cui, C.-B., Kakeya, H., Osada, H., Novel mammalian cell cycle inhibitors, spirotryprostatins A and B, produced by Aspergillus fumigatus, which inhibit mammalian cell cycle at G2/M phase, Tetrahedron, 52, 12651-12666, 1996.

Da Silva, J. F., Garden, S. J., Pinto, A. C., The chemistry of isatins: a review from 1975 to 1999, Journal of the Brazilian Chemical Society, 12, 273-324, 2001.

Dabiri, M., Bahramnejad, M., Baghbanzadeh, M., Ammonium salt catalyzed multicomponent transformation: simple route to functionalized spirochromenes and spiroacridines, Tetrahedron, 65, 9443-9447, 2009.

Damyanova, S., Grange, P., Delmon, B., Surface characterization of zirconia-coated alumina and silica carriers, Journal of catalysis, 168, 421-430, 1997.

Dandia, A., Jain, A. K., Bhati, D. S., NaCl as a novel and green catalyst for the synthesis of biodynamic spiro heterocycles in water under sonication, Synthetic communications, 41, 2905-2919, 2011.

Galliford, C. V., Scheidt, K. A., Pyrrolidinyl-Spirooxindole Natural Products as Inspirations for the Development of Potential Therapeutic Agents, Angewandte Chemie International Edition, 46, 8748-8758, 2007.

Gao, S., Tsai, C. H., Tseng, C., Yao, C.-F., Fluoride ion catalyzed multicomponent reactions for efficient synthesis of 4H-chromene and N-arylquinoline derivatives in aqueous media, Tetrahedron, 64, 9143-9149, 2008.

Gladysz, J. A., Introduction: Recoverable catalysts and reagents perspective and prospective, Chemical reviews, 102, 3215-3216, 2002.

Gladysz, J. A., Recoverable catalysts. Ultimate goals, criteria of evaluation, and the green chemistry interface, Pure and Applied Chemistry, 73, 1319-1324, 2001.

Grunes, J., Zhu, J., Somorjai, G. A., Catalysis and nanoscience, Chemical Communications, 2257-2260, 2003.

Hari, G. S., Lee, Y. R., Efficient one-pot synthesis of spirooxindole derivatives by ethylenediamine diacetate catalyzed reactions in water, Synthesis, 2010, 453-464, 2010.

He, D., Ding, Y., Luo, H., Li, C., Effects of zirconia phase on the synthesis of higher alcohols over zirconia and modified zirconia, Journal of Molecular Catalysis A: Chemical, 208, 267-271, 2004.

Jafarpour, M., Rezapour, E., Ghahramaninezhad, M., Rezaeifard, A., A novel protocol for selective synthesis of monoclinic zirconia nanoparticles as a heterogeneous catalyst for condensation of 1, 2-diamines with 1, 2-dicarbonyl compounds, New Journal of Chemistry, 38, 676-682, 2014.

James, S. L., Adams, C. J., Bolm, C., Braga, D., Collier, P., Friščić, T., Grepioni, F., Harris, K. D., Hyett, G., Jones, W., Mechanochemistry: opportunities for new and cleaner synthesis, Chemical Society Reviews, 41, 413-447, 2012.

Jiang, X., Sun, Y., Yao, J., Cao, Y., Kai, M., He, N., Zhang, X., Wang, Y., Wang, R., Core Scaffold-Inspired Concise Synthesis of Chiral Spirooxindole-Pyranopyrimidines with Broad-Spectrum Anticancer Potency, Advanced Synthesis & Catalysis, 354, 917-925, 2012.

Kang, T.-H., Matsumoto, K., Tohda, M., Murakami, Y., Takayama, H., Kitajima, M., Aimi, N., Watanabe, H., Pteropodine and isopteropodine positively modulate the function of rat muscarinic M 1 and 5-HT 2 receptors expressed in Xenopus oocyte, European journal of pharmacology, 444, 39-45, 2002.

Karmakar, B., Nayak, A., Banerji, J., A clean and expedient synthesis of spirooxindoles in aqueous media catalyzed over nanocrystalline MgO, Tetrahedron Letters, 53, 5004-5007, 2012.

Khodakov, A., Olthof, B., Bell, A. T., Iglesia, E., Structure and catalytic properties of supported vanadium oxides: support effects on oxidative dehydrogenation reactions, Journal of catalysis, 181, 205-216, 1999.

Kidwai, M., Jahan, A., Mishra, N. K., Gold (III) chloride (HAuCl 4· 3H 2 O) in PEG: a new and efficient catalytic system for the synthesis of functionalized spirochromenes, Applied Catalysis A: General, 425, 35-43, 2012.

Lashgari, N., Ziarani, G. M., Synthesis of heterocyclic compounds based on isatin through 1, 3-dipolar cycloaddition reactions, Arkivoc, 1, 277-320, 2012.

Li, W., Liu, H., Iglesia, E., Structures and properties of zirconia-supported ruthenium oxide catalysts for the selective oxidation of methanol to methyl formate, The Journal of Physical Chemistry B, 110, 23337-23342, 2006.

Li, Y., Chen, H., Shi, C., Shi, D., Ji, S., Efficient one-pot synthesis of spirooxindole derivatives catalyzed by L-proline in aqueous medium, Journal of combinatorial chemistry, 12, 231-237, 2010.

Liu, G., Lin, Y., Electrochemical sensor for organophosphate pesticides and nerve agents using zirconia nanoparticles as selective sorbents, Analytical Chemistry, 77, 5894-5901, 2005.

Liu, S., Han, M. Y., Silica-Coated Metal Nanoparticles, Chemistry–An Asian Journal, 5, 36-45, 2010.

Longeon, A., Guyot, M., Vacelet, J., Araplysillins-I and-II: Biologically active dibromotyrosine derivatives from the spongePsammaplysilla arabica, Experientia, 46, 548-550, 1990.

Lu, J., Zang, J., Shan, S., Huang, H., Wang, Y., Synthesis and characterization of core− shell structural MWNT− zirconia nanocomposites, Nano letters, 8, 4070-4074, 2008.

Luo, X., Morrin, A., Killard, A. J., Smyth, M. R., Application of nanoparticles in electrochemical sensors and biosensors, Electroanalysis, 18, 319-326, 2006.

Mercera, P., Van Ommen, J., Doesburg, E., Burggraaf, A., Ross, J., Zirconia as a Support for Catalysts: Evolution of the Texture and Structure on Calcination in Air, Applied catalysis, 57, 127-148, 1990.

Mortikov, V. Y., Litvinov, Y. M., Shestopalov, A., Rodinovskaya, L., Shestopalov, A., Versatile three-component synthesis of 2′-amino-1, 2-dihydrospiro [(3H)-indole-3, 4′-(4′ H)-pyran]-2-ones, Russian Chemical Bulletin, 57, 2373-2380, 2008.

Pacchioni, G., Quantum chemistry of oxide surfaces: from CO chemisorption to the identification of the structure and nature of point defects on MgO, Surface Review and Letters, 7, 277-306, 2000.

Polshettiwar, V., Baruwati, B., Varma, R. S., Self-assembly of metal oxides into three-dimensional nanostructures: synthesis and application in catalysis, Acs Nano, 3, 728-736, 2009.

Polshettiwar, V., Nadagouda, M. N., Varma, R. S., The synthesis and applications of a micro-pine-structured nanocatalyst, Chemical Communications, 6318-6320, 2008.

Polshettiwar, V., Varma, R. S., Green chemistry by nano-catalysis, Green Chemistry, 12, 743-754, 2010.

Ramarao, C., Ley, S. V., Smith, S. C., Shirley, I. M., DeAlmeida, N., Encapsulation of palladium in polyurea microcapsules, Chemical Communications, 1132-1133, 2002.

Rao, B. M., Reddy, G. N., Reddy, T. V., Devi, B. P., Prasad, R., Yadav, J., Reddy, B. S., Carbon–SO 3 H: a novel and recyclable solid acid catalyst for the synthesis of spiro [4H-pyran-3, 3′-oxindoles], Tetrahedron Letters, 54, 2466-2471, 2013.

Rashad, M., Baioumy, H., Effect of thermal treatment on the crystal structure and morphology of zirconia nanopowders produced by three different routes, journal of materials processing technology, 195, 178-185, 2008.

Reetz, M. T., Westermann, E., Phosphane-free palladium-catalyzed coupling reactions: the decisive role of Pd nanoparticles, Angewandte Chemie International Edition, 39, 165-168, 2000.

Rhodes, M. D., Bell, A. T., The effects of zirconia morphology on methanol synthesis from CO and H2 over Cu/ZrO2 catalysts: Part I. Steady-state studies, Journal of catalysis, 233, 198-209, 2005.

Shanthi, G., Subbulakshmi, G., Perumal, P. T., A new InCl 3-catalyzed, facile and efficient method for the synthesis of spirooxindoles under conventional and solvent-free microwave conditions, Tetrahedron, 63, 2057-2063, 2007.

Sholklapper, T. Z., Radmilovic, V., Jacobson, C. P., Visco, S. J., De Jonghe, L. C., Synthesis and stability of a nanoparticle-infiltrated solid oxide fuel cell electrode, Electrochemical and solid-state letters, 10, B74-B76, 2007.

Sridhar, R., Srinivas, B., Madhav, B., Reddy, V. P., Nageswar, Y. V. D., Rao, K. R., Multi-component supramolecular synthesis of spirooxindoles catalyzed by β-cyclodextrin in water, Canadian Journal of Chemistry, 87, 1704-1707, 2009.

Steiner III, S. A., Baumann, T. F., Bayer, B. C., Blume, R., Worsley, M. A., MoberlyChan, W. J., Shaw, E. L., Schlögl, R., Hart, A. J., Hofmann, S., Nanoscale zirconia as a nonmetallic catalyst for graphitization of carbon and growth of single- and multiwall carbon nanotubes, Journal of the American Chemical Society, 131, 12144-12154, 2009.

Stichert, W., Schüth, F., Kuba, S., Knözinger, H., Monoclinic and tetragonal high surface area sulfated zirconias in butane isomerization: CO adsorption and catalytic results, Journal of catalysis, 198, 277-285, 2001.

Trost, B. M., Brennan, M. K., Asymmetric syntheses of oxindole and indole spirocyclic alkaloid natural products, Synthesis, 2009, 3003-3025, 2009.

Tsipouriari, V., Efstathiou, A., Zhang, Z., Verykios, X., Reforming of methane with carbon dioxide to synthesis gas over supported Rh catalysts, Catalysis today, 21, 579-587, 1994.

Varma, R. S., Chemical activation by mechanochemical mixing, microwave and ultrasonic irradiation, Green Chemistry, 10, 1129-1130, 2008.

Wang, L.-M., Jiao, N., Qiu, J., Yu, J.-J., Liu, J.-Q., Guo, F.-L., Liu, Y., Sodium stearate-catalyzed multicomponent reactions for efficient synthesis of spirooxindoles in aqueous micellar media, Tetrahedron, 66, 339-343, 2010.

Xie, S., Iglesia, E., Bell, A. T., Water-assisted tetragonal-to-monoclinic phase transformation of ZrO2 at low temperatures, Chemistry of materials, 12, 2442-2447, 2000.

Yamaguchi, T., Application of ZrO2 as a catalyst and a catalyst support, Catalysis today, 20, 199-217, 1994.

Zhu, S.-L., Ji, S.-J., Zhang, Y., A simple and clean procedure for three-component synthesis of spirooxindoles in aqueous medium, Tetrahedron, 63, 9365-9372, 2007.

Illustrations

Nmr spectra of representative compounds

Ethyl 7'-amino-5-chloro-2,2',4'-trioxo-1',2',3',4'-tetrahydrospiro[indoline-3,5'-pyrano[2,3-d]pyrimidine]-6'-carboxylate (4a)

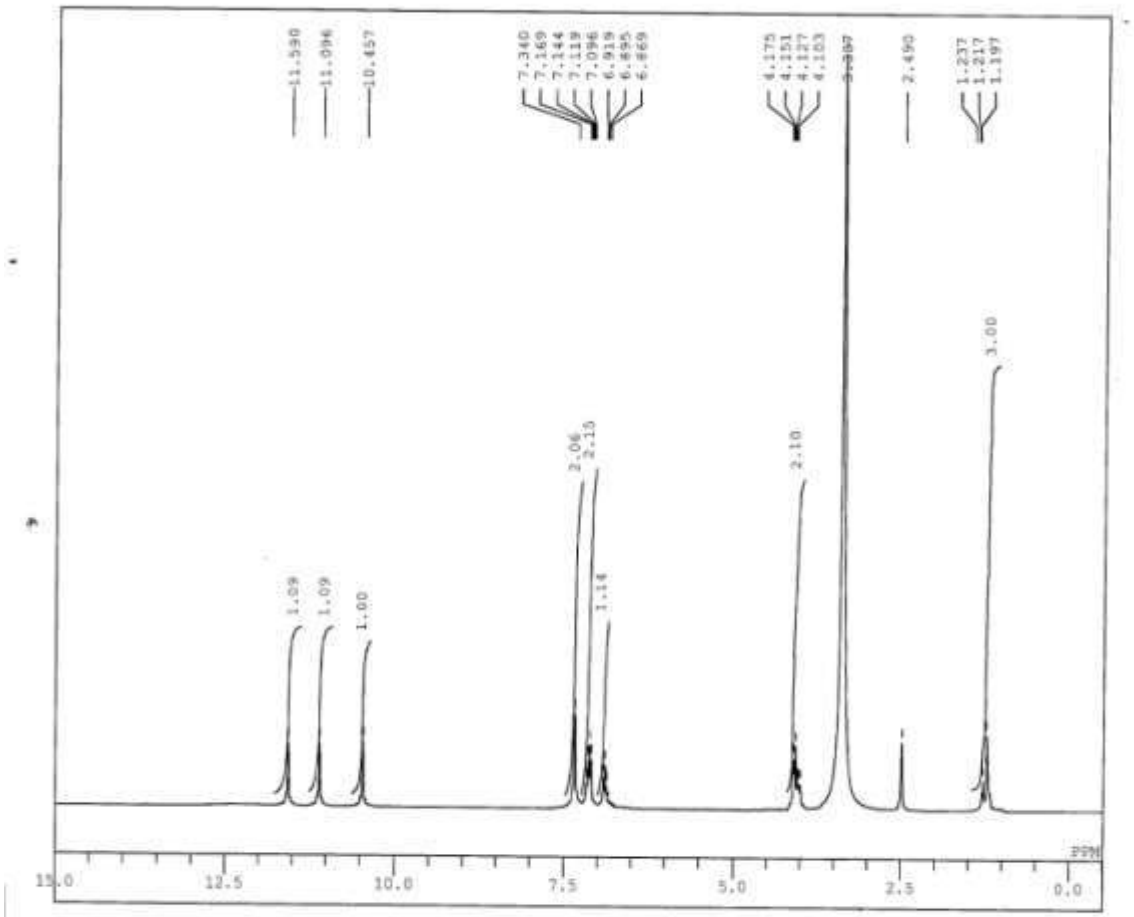

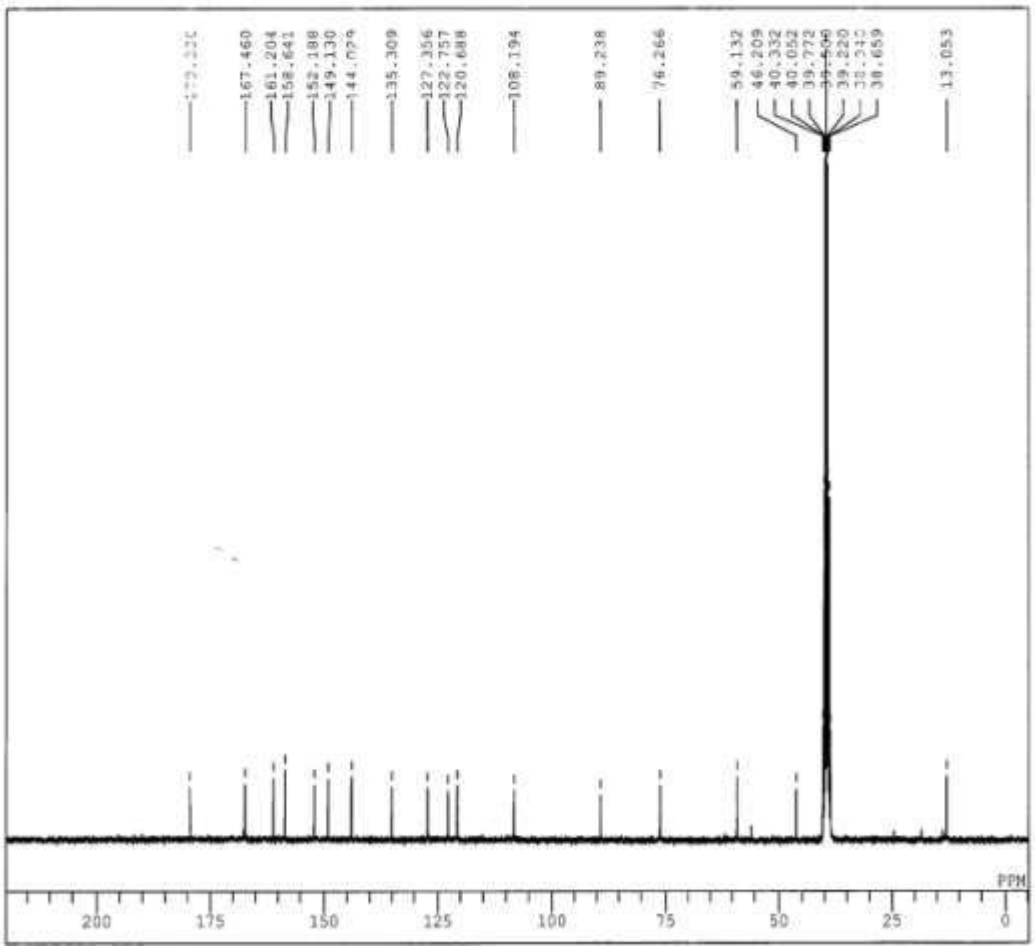
167.460
161.204
158.641
152.188
149.130
144.709
135.309
127.356
122.757
120.688
108.194
89.238
76.266
59.132
46.209
40.332
40.052
39.772
39.220
38.659
13.053
PPM
200
175
150
125
100
75
50
25
0

Ethyl 2-amino-1'-ethyl-7,7-dimethyl-2',5-dioxo-5,6,7,8-tetrahydrospiro [chromene-4,3'-indoline]-3-carboxylate (4i)

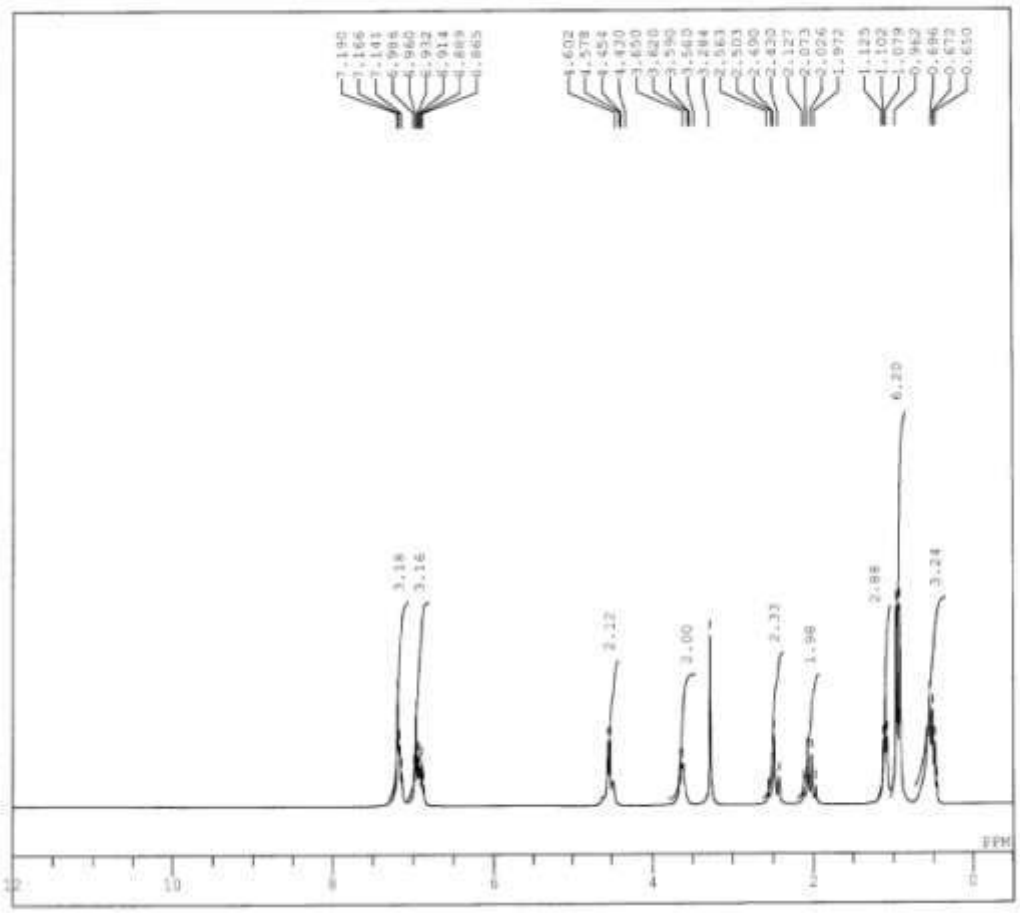

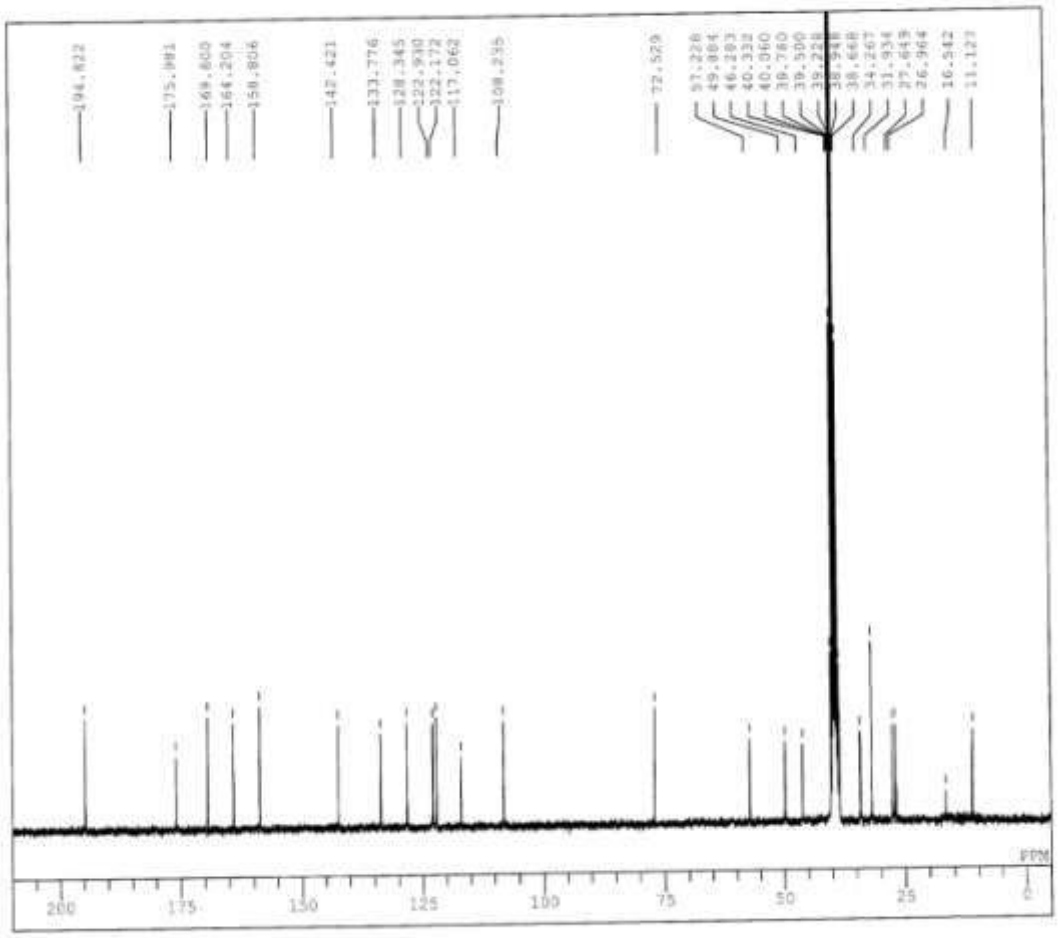
194.622
175.981
169.800
164.204
150.806
142.421
133.776
128.345
122.930
122.172
117.062
108.235
72.529
57.226
49.864
46.293
40.332
40.060
39.780
39.500
39.228
38.948
38.668
34.267
31.934
25.649
26.964
16.542
11.123
PPM
200
175
150
125
100
75
50
25
0

Ethyl 7'-amino-1-ethyl-2',2'-dimethyl-2,4'-dioxo-4'H-spiro[indoline-3,5'-pyrano[2,3-d][1,3]dioxine]-6'-carboxylate (4n)

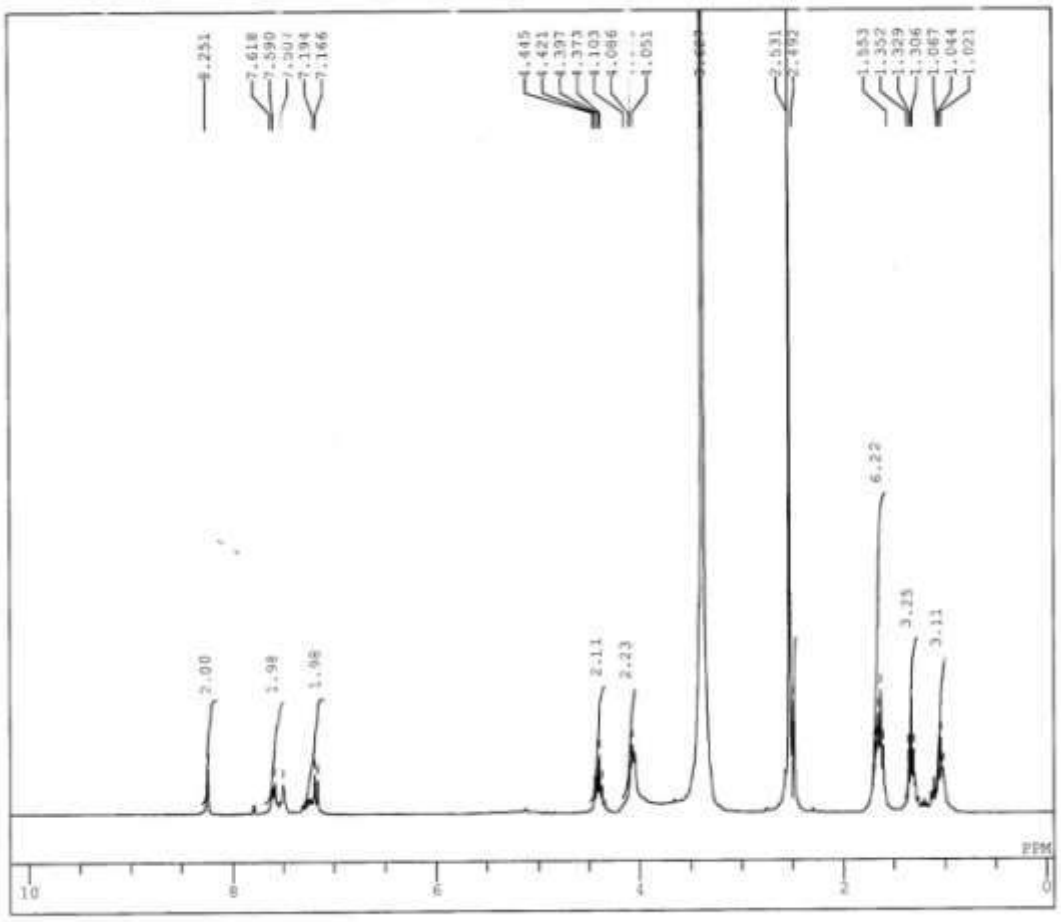

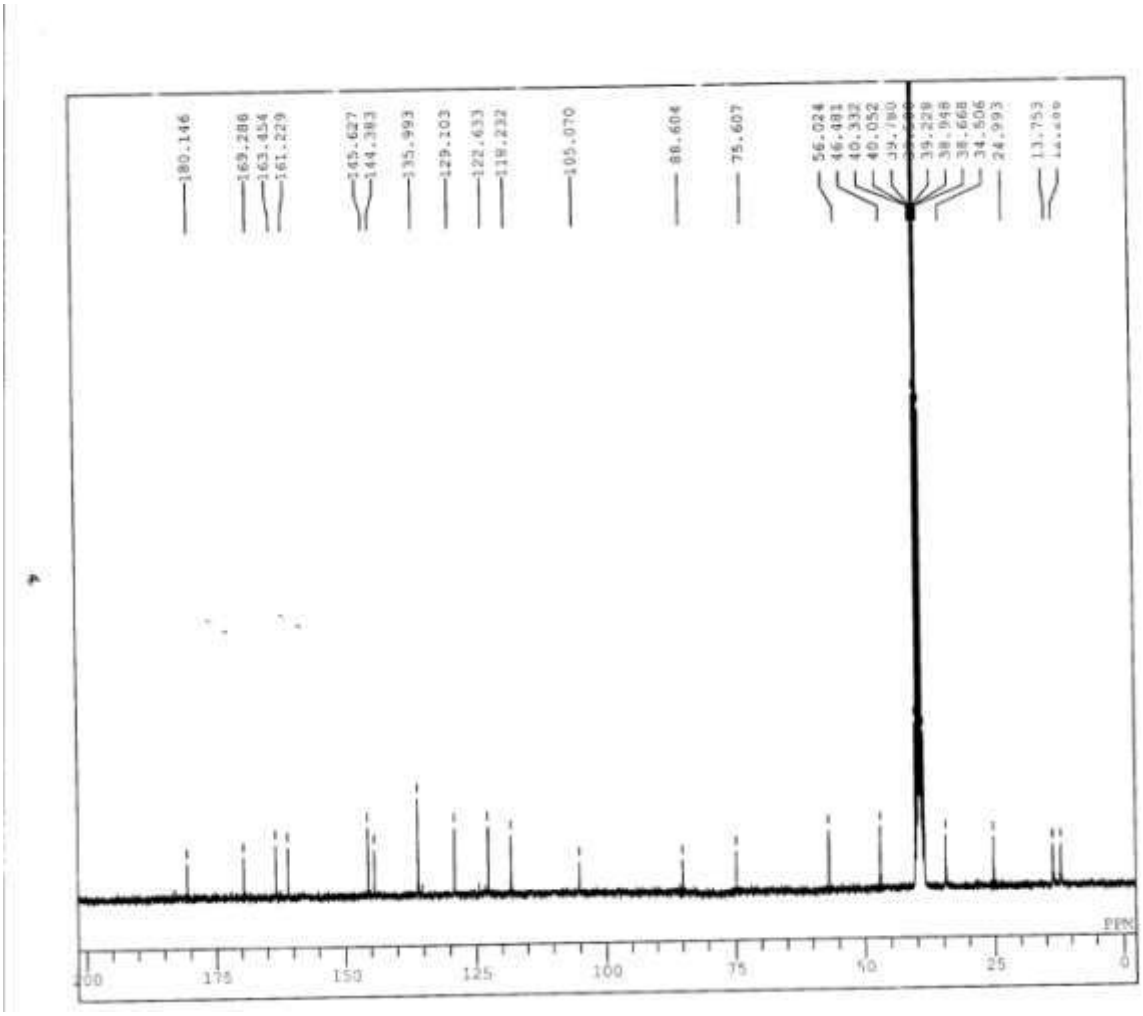
180.146
169.286
163.454
161.229
145.627
144.383
135.993
129.203
122.633
119.232
105.070
86.604
75.607
56.024
46.481
40.332
40.052
39.229
38.948
38.668
34.606
24.993
13.753
PPM
200
175
150
125
100
75
50
25
0